Characterizing the Molecular Gas in Infrared Bright Galaxies with CARMA

2024/11/20

Alatalo et al. 2024, arXiv:2409.09116v1

Introduction

- Galaxies interactions play an important role in the evolution of galaxies
- Simulations of galaxy interactions
  "The galactic coalescence causes a starburst → igniting the central SMBH → blowing away the surrounding gas by outflow"
- Does AGN outflow really deplete gas in the galaxy?
- How molecular gases change during mergers?

➢ Ideal sample for studying molecular gases in the merger phase: **GOALS sample** (Armus et al. 2009)

➢ Much of the previous work has focused on galaxies with high infrared luminosity ($L_{IR} \lesssim 10^{11.5} L_{\odot}$)

Sample

- **28 objects** cross-matched with GOALS sample and CARMA archive (contained observations for the CO(1-0) line and requiring complete velocity coverage of the line)
- IR luminosity range: $10^{11.1-12.5}\ L_{\odot}$
- Wide range of interaction phase

Observations and Analysis

- CARMA observations: July 2008 - June 2014
- The field of view of these observations corresponds to the primary beam of the 6m antennas at 3mm of ≈ 100''
- 16 of 28 galaxies were detected 100 GHz continuum
- Stellar mass, dust mass, star formation rate of each object were derived by SED fitting using MAGPHYS and SED3FIT (if there are signs of an AGN)
  - Photometric data: GALEX, optical, 2MASS, Spitzer
- Measuring AGN contribution using MIR emission (Petric et al. 2011)

Discussion

100 GHz SFRs vs SED fit SFRs

- For most objects, the SFR at 100 GHz exceeds the MAGPHYS SFR by a factor of 2 to 50.
- AGN contributions were found in 12 objects

➢ Much of the 100 GHz emission is AGN origin (or Rayleigh-Jeans tail of dust emission)

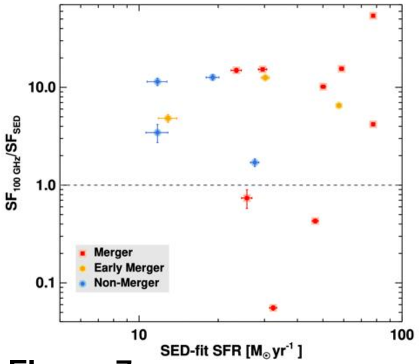

Figure 7.

Molecular gas fraction

$$f_{mol} = \frac{M_{mol}}{M_{mol} + M_{*}}$$

- Molecular gas fraction correlates with star formation rate
  →The more molecular gas, the more star formation occurs naturally.
- Molecular gas fraction correlates with merger stage

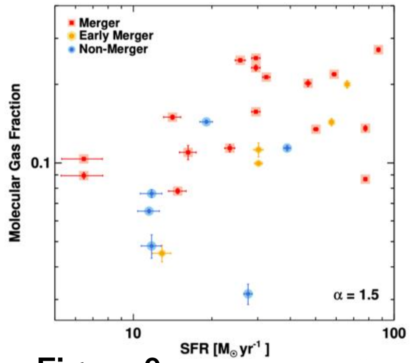

Figure 9.

- Many systems in CARMA GOALS exhibit velocity gradients despite their interactions.

➢ the order gradients observed in molecular gases do not imply order rotation in the system.

➢ the disruption in the molecular gas is not entirely consistent with the optical or infra-red morphological features of the system.

- Using $\alpha = 1.5$, gas-to-dust ratios span a more reasonable range of values
- Median gas to dust ratio
  Merger (444), Early merger (368), Non-merger (254)

➢ Suggests that dust may be destroyed and molecular gases diffused through the interaction

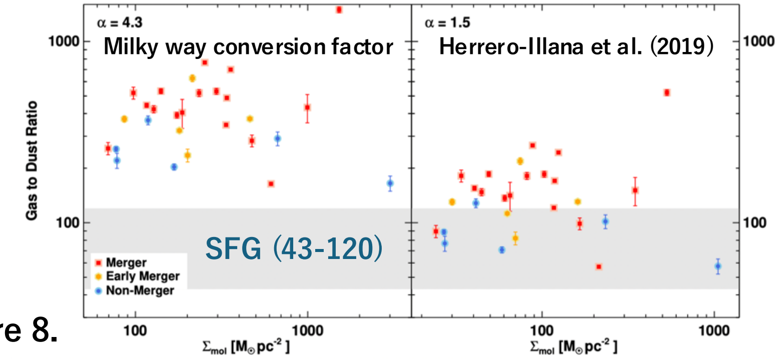

Figure 8.

Schmidt–Kennicutt relation

- The CARMA GOALs sources have an enhanced star formation efficiency

➢ Increased turbulence in these systems and decreased free-fall times compared to star-forming galaxies may have resulted in increased star formation efficiency.

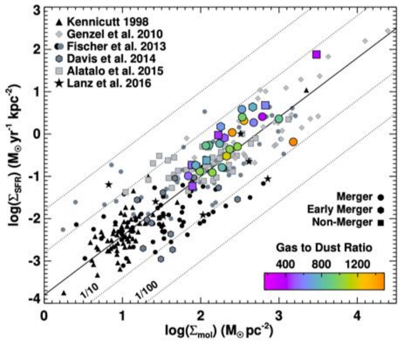

Figure 11. The Schmidt-Kennicutt relation (Kennicutt 1998) for the CARMA GOALS sample (color-coded by gas-to-dust ratio), with comparisons to normal star-forming galaxies (black triangles; Kennicutt 1998 and black circles; Fisher et al. 2013), bulges (gray circles; Fisher et al. 2013), early-type galaxies (teal squares; Davis et al. 2014), Hickson Compact Group galaxies (blue hexagons; Alatalo et al. 2015c), high-redshift galaxies (gray diamonds; Genzel et al. 2010), and radio galaxies (black squares; Ogle et al. 2010). The diagonal lines represent the 10× and 100× deviations from the average relation. All star formation rates have been normalized to the Chabrier initial mass function (Chabrier 2003).

- Multiple objects show evidence of extended line wings

➢ Suggests the presence of molecular outflows in many objects - Some objects have confirmed AGN-driven molecular outflows

➢ Molecular outflows are not a dominant mechanism in expelling the molecular gas (Penaloza et al. 2023)

➢ AGN jet → depletion of the gas reservoir via star formation

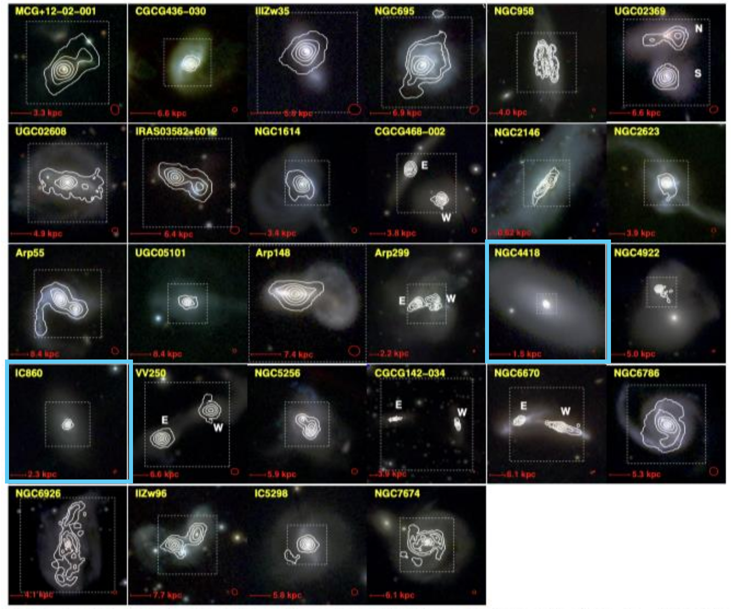

Figure 1. The CO(1–0) integrated intensity (moment0) maps from CARMA (white contours) are overlaid on the 3-color *g r i* images from PanSTARRS (Chambers et al. 2016) for the 28 CARMA GOALS galaxies, ordered based on their RA. For each map, north is up and east is to the left. The red bar in the lower lefthand corner demarcates 10″ in each field (with the corresponding physical scale listed). The beam is shown in the lower right corner in red. The gray dotted borders represent the size of the CO-only moments from Figure 2 and 3.

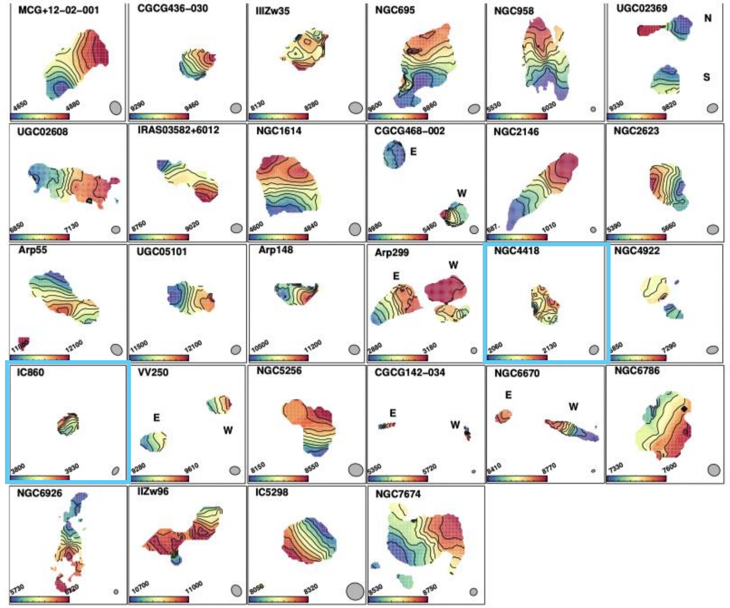

Figure 3. The mean velocity (moment1) maps of CO(1–0) of the 28 CARMA GOALS galaxies. The size scales are identical to those used in Figure 2.

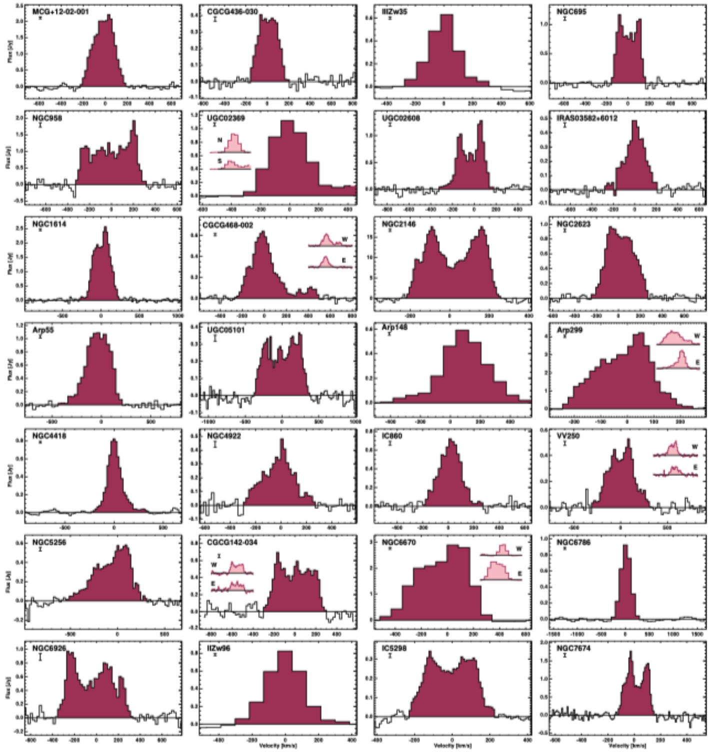

Figure 4. The integrated CO(1–0) spectra for the 28 CARMA GOALS galaxies. Each spectrum was created by using the moment0 map (shown in Fig. 2) as a clip mask and totaling all flux within the mask in each channel. The areas shaded in fuschia denote the channels used to calculate the total flux. The RMS noise per channel is shown in the upper left corner below the galaxy name. In all cases, the CO(1–0) is detected to be very high signal to noise. The six CARMA objects (UGC 02369, CGCG 468-002, Arp 299, VV 250, CGCG 142-034, and NGC 6670), where two different galaxies were differentiable in our data have had their spectra separated and plotted in the corner of the panel.

Petric et al. 2018

Merger stages

Non-mergers (nm): targets without obvious signs of morphological disturbances

Early mergers (em): systems in which the interacting galaxies are within 1 arcmin of each other but show little or no morphological disturbance

Mergers (m): includes all other stages of gravitational interaction.

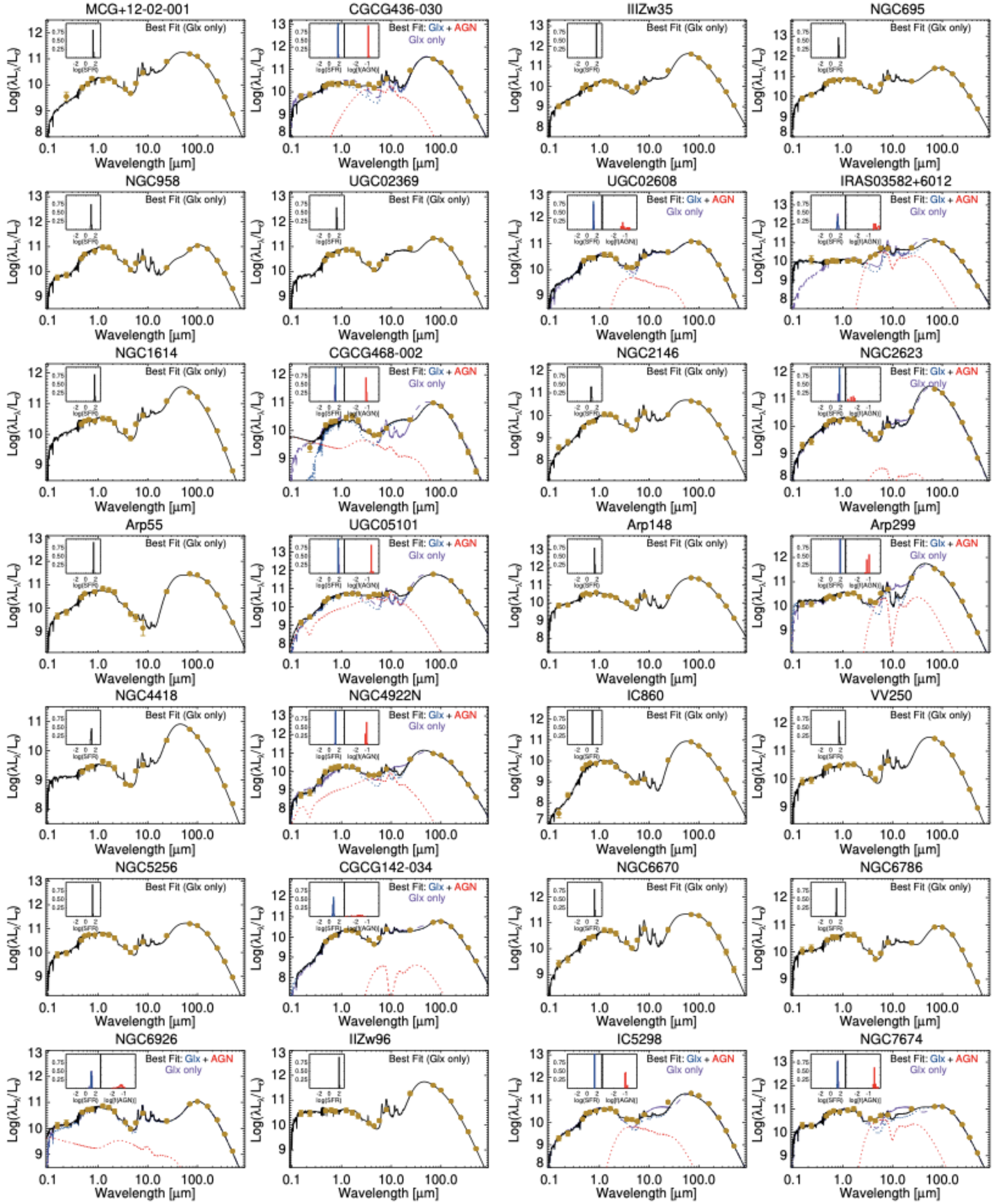

Figure 6. Best-fitting models to the SEDs. The black line shows the best overall model. In some cases, the fit was improved by including a torus component from the AGN (shown in red) in addition to the galactic emission (shown in blue). The fit achieved with just galactic emission in those cases is shown in purple. See Section 3.3 for discussion on the fitting process. Probability density functions (PDFs) for SFR in the last 10 Myr and, as relevant, fraction of infrared luminosity arising from the AGN component are shown as insets. When a galaxy is modeled both with and without an AGN component, both of the resulting SFR PDFs are shown. These generally do not show much difference, indicating that the inclusion of an AGN component does not affect our derived SFR significantly.